

Chemically active substitutional nitrogen impurity in carbon nanotubes

Andriy H. Nevidomskyy, Gábor Csányi, and Michael C. Payne

*Theory of Condensed Matter group, Cavendish Laboratory,
University of Cambridge, Cambridge CB3 0HE, UK*

(Dated: February 7, 2020)

We investigate the nitrogen substitutional impurity in semiconducting zigzag and metallic armchair single-wall carbon nanotubes using *ab initio* density functional theory. In the high concentration regime (1 at.%) our results agree with previous calculations, and even an originally semiconducting tube is predicted to become metallic. At lower concentrations however, the defect state in a zigzag tube becomes spatially localized, and develops a flat energy level in the band gap. Such a localized state makes the impurity site chemically and electronically active. We find that if two neighbouring tubes have their impurities facing each other, an inter-tube covalent bond forms. This finding opens an intriguing possibility for tunnel junctions, as well as the functionalization of suitably doped carbon nanotubes by selectively forming chemical bonds with ligands at the impurity site.

PACS numbers: 61.46.+w, 81.07.De, 73.22.-f

Ever since their discovery[1, 2], carbon nanotubes (CNT) have been heralded as the new wonder-material of the future. Their remarkable mechanical and electronic properties destine them to play a major role in all kinds of nanotechnologies and molecular electronics. At least two major hurdles have to be overcome in order to fulfill this potential. First, manipulation of individual tubes is at best difficult today, which prevents mass production of devices. Second, the ability to fine-tune the various properties of the material to suit particular applications has to be achieved.

Carbon nanotubes exhibit a variety of electronic properties, for example, depending on their diameter and chirality, they vary from being metallic to semiconducting[3]. The presence of defects and impurities that are electronically or chemically active can change these properties and thus have a significant bearing on a broad range of applications. In this paper we investigate the nitrogen substitutional impurity in single-wall carbon nanotubes. In the case of semiconducting tubes, doping with electrons or holes is the principle route to making electronic devices. Alternatively, introducing new levels in the bandgap with associated electronic states that are spatially localized, can create chemically active impurity sites.

Several groups have produced nanotubes containing nitrogen [4, 5, 6, 7, 8, 9, 10, 11, 12, 13, 14] or nitrogen and boron[5, 15, 16]. All of these were multiwall tubes, except for [16], where nitrogen was always accompanied by boron. The measured atomic concentrations of the impurities were relatively high in all cases, above 1%, and all the CN_x tubes were found to be metallic, as predicted by both empirical and *ab initio* theoretical models[10, 11, 17]. Indeed, one other reason for the particular interest in CN_x tubes was that they might make even initially semiconducting tubes metallic.

Various structural models have been proposed for the incorporation of nitrogen into the carbon network. Di-

rect substitution was first studied by Yi and Bernholc[18] using density functional theory at an atomic impurity concentration of about 1%, where they found an impurity state lying 0.27 eV below the bottom of the conduction band at the Γ point and a significant overlap of the states associated with the adjacent nitrogens (8.4 Å apart). Lammert *et al.*[19] considered disordered substitution of boron and nitrogen at a concentration of 3.5% and 1.4% using the self consistent tight binding method. They observed both donor and acceptor levels in the gap. For an isolated nitrogen or boron impurity, they found the impurity state to be localized within about 10 Å for an (8,0) tube.

Another atomic arrangement for the experimentally observed nitrogen impurity was proposed by Terrones *et al.*[6], where they suggest that at high concentrations (above about 10%) nitrogens are divalent, pyridine-like. Later publications from the same group refine this model and correlate the calculated density of states of metallic tubes with experimental observations [10, 11]. A number of studies[17, 20] were also devoted to the transport properties of nitrogen doped metallic nanotubes.

To study the isolated substitutional nitrogen defect, the simulation cell has to be as long as possible. The existing constraints of computational power mean that the diameter of the tube should therefore be as small as possible. In all calculations we used the achiral zigzag (8,0) and armchair (5,5) nanotubes. Our simulation cell has periodic boundary conditions, the tubes are arranged parallel to the z axis and form a triangular lattice in the perpendicular x–y plane. This arrangement is experimentally seen in carbon nanotube ropes[3]. The unit cell of the undoped zigzag (armchair) tube consists of 32 (20) carbon atoms and is 4.22 Å (2.46 Å) long. In the following, we refer to this as our basic building block, when we construct simulation cells. We studied a range of nitrogen concentrations from 0.26% to 1% by introducing one impurity atom and changing the size of the simulation

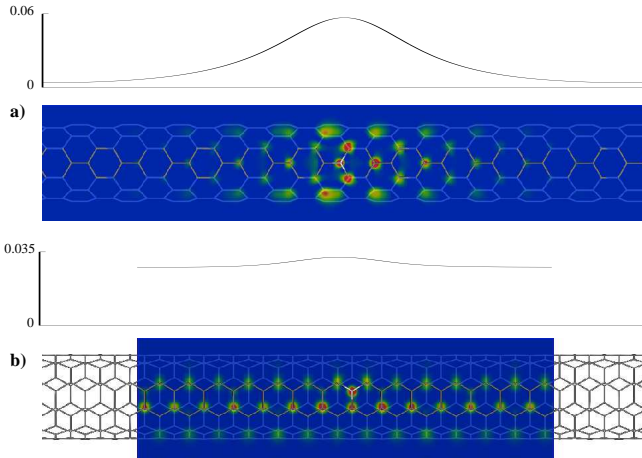


FIG. 1: Slice of the spin density of the N-doped carbon nanotube in a plane parallel to the tube axis, the plane being tangential to the tube at the position of the nitrogen ion, for a) (8,0) zigzag tube, comprising 12 unit cells (50.6 Å), and b) (5,5) armchair tube, comprising 14 unit cells (34.3 Å). Above each slice, we plot the envelope of the spin density (integrated in the plane perpendicular to the tube) in the units of electron/Å. The nitrogen ion is marked white. The colour range maps the value of the spin density, with blue corresponding to the smallest and red to the highest values. Note that the scale of the spin density is quite different for the two panels.

cell along the axis of the tube. The largest simulation cell contained 12 unit cells along the z axis for the zigzag tube and 14 unit cells for the armchair tube, respectively, with one impurity atom in it.

Throughout, we used *ab-initio* plane-wave pseudopotential density functional theory[21] as implemented in the CASTEP code[22]. The generalized gradient approximation was used to account for exchange and correlation in the Perdew–Burke–Ernzerhof form[23]. All calculations were spin-polarized and ultrasoft pseudopotentials were used for carbon and nitrogen with a cutoff energy of 300 eV. We assessed the adequacy of this cutoff by performing calculations at 350 eV for the smallest unit cells and verified that none of properties reported in this work changed perceptibly. For each concentration, the ionic positions were optimized by using one k-point at the Γ point for the largest simulation cells, and correspondingly more k-points for the smaller cells. After the geometry optimization has converged, the band structure was calculated using a finer mesh of k-points.

We find that the equilibrium position of the nitrogen ion is almost unchanged with respect to the corresponding C atom in the undoped nanotube, being moved by at most 0.01 Å, similarly to the case of azafullerene, $C_{59}N$ [24, 25]. A slice of the calculated spin-density for both zigzag and armchair cases is shown in Fig. 1. The spin density is maximal on the N ion and the neighbour-

ing C ions and shows oscillatory behaviour as it reaches a local maximum on every other ion in the network, again similarly to that observed in $C_{59}N$ [24, 25]. The shape of the spin density isosurfaces is reminiscent of the π -orbitals in graphite with their axes of symmetry perpendicular to the sheet. The oscillatory behaviour can be understood in terms of the RKKY formalism. Conventionally applied to metals, a magnetic impurity is shown to polarize the electron cloud in such a way that the charge density oscillates as a function of distance away from the impurity with a wave vector of $2k_F$. In case of graphite, the Fermi surface becomes just a point at the edge of the Brillouin zone, so the real space periodicity corresponding to $2k_F$ is easily seen to be the distance across a hexagon, which is the same as the length of the primitive lattice vector. In our case, the spin of the extra electron on the nitrogen atom similarly polarizes the rest of the electrons, and we see the same oscillations for both the metallic and the semiconducting tube. Interestingly, in both carbon nanotubes and graphite sheet substitutionally doped with nitrogen, the spin density virtually never becomes negative, in contrast to the behaviour in $C_{59}N$ where the spin density oscillates symmetrically around zero.

A crucial difference between the armchair and the zigzag tubes is that the introduction of the nitrogen atom breaks the left–right mirror symmetry in the latter case. As two impurity atoms approach each other in an armchair tube, their interaction will show oscillatory behaviour depending on whether the spin density maxima induced by the respective nitrogens coincide or not. But in the zigzag tube the local maxima of the spin density occur on different sublattices on the two sides of the nitrogen atom. As two impurities approach, their respective spin density maxima never coincide, irrespective of whether the nitrogens occupy the same sublattice or not.

The localization of the extra electron associated with the isolated impurity shows a striking difference between the metallic and semiconducting cases, despite the fact that the band gap of the latter is quite small (0.6 eV according to the DFT calculations). In the armchair tube, the unpaired electron is almost completely delocalized along the tube, as can be seen from the plot of the envelope of the spin density in the lower panel of Fig. 1. However, for the zigzag tube, it is localized near the impurity site, but the localization region is fairly large, about 20 Å. This region contains about 80% of the unpaired spin density, a region 30 Å long contains 90%. The decaying envelope of the spin density is exponential.

Figure 2 shows the band structure of the nitrogen-doped nanotubes along with the corresponding densities of states. The band structure of undoped tube (folded in such a way, that it fits into the shrunk Brillouin zone corresponding to the larger supercell) is shown for comparison. For the zigzag case, the extra band of the impurity falls somewhere near the bottom of the conduc-

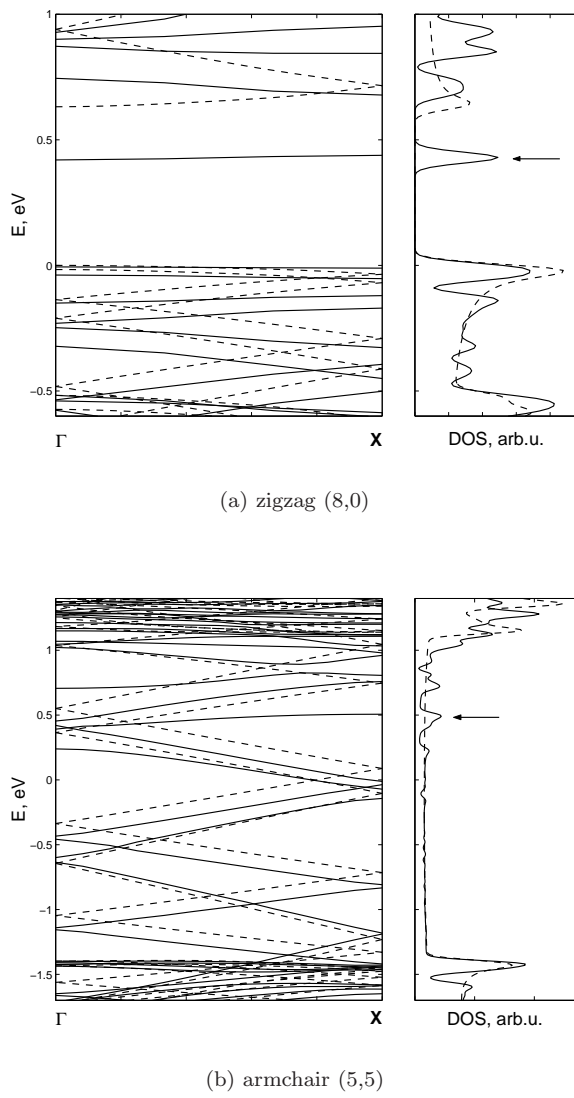


FIG. 2: Band structures and corresponding densities of states for the largest N-doped carbon nanotubes studied (solid line) versus the folded band structure of pure nanotube (dashed line) in a) (8,0) zigzag nanotube, bands aligned in such a way that the valence band edge coincides with that of pure nanotube, and b) (5,5) armchair tube, bands aligned in such a way that the van Hove singularities below the Fermi level coincide. The arrows mark the new band associated with the impurity. For reasons of clarity we only show the up-spin channel, which contains the unpaired electron. Note that below the Fermi level, the splitting of the spin channels is less than 0.03 eV.

tion band, and a complicated hybridization takes place with the existing unoccupied bands. The end result is that a new flat level appears about 0.2 eV below the bottom of the conduction band. This impurity level exhibits itself as a sharp peak in the density of states. The rest of the low lying conduction bands also rearrange thereby

showing additional peaks in the density of states. Note that the lowest dispersive conduction band, lying directly above the impurity band, curves downwards from the Γ point, rather than upwards as in the undoped tube. As the concentration of nitrogen is increased, the impurity level acquires significant dispersion, until at 0.6%, it overlaps with the conduction bands. Interestingly, the size of the band gap increases by more than 20% during this transition. In the armchair tube, the impurity introduces a peak at about 0.6 eV below the first van Hove singularity above the Fermi level. There are a number of additional peaks as well, which are formed because of the hybridization and level repulsion taking place between the energy levels of impurity and pristine nanotube.

The localized electronic state of the semiconducting tube offers the intriguing possibility of being chemically active and forming covalent bonds with ligands or other tubes. Figure 3 shows two zigzag nanotubes each doped with nitrogen in such a way that two carbon atoms with originally significant spin density on them face each other. As the charge density slice shows, a covalent bond is formed between these atoms, and thus the tubes. The two carbon atoms pop out of the tangent plane of the tubes, and take up an sp^3 configuration, the bond length between them being 1.65 Å.

The further corroboration of the formation of the covalent bond between the carbon atoms comes from the analysis of the charge density originating from different orbitals. Such analysis has shown that the largest contribution to the total charge density between the newly bonded carbon atoms comes from the HOMO orbital. It should be noted that the valence and conduction bands of our system overlap slightly and thus when talking about the HOMO orbital we mean the highest partially occupied energy band. In this case the HOMO band is occupied by about 0.3 of an electron. Such an intertube bond can potentially affect the mechanical properties of suitably doped carbon nanotube bundles, or can enhance the tunneling between the tubes. Note that in order to obtain the geometry shown, the two tubes were slightly pressed against each other, which is realistic when modelling a nanotube lying on top of another on a surface[26].

We performed *ab initio* calculations of zigzag and armchair carbon nanotubes substitutionally doped with nitrogen. In the case of the armchair nanotube, the impurity state is totally delocalized and the corresponding energy level falls inside the unoccupied bands of the pristine nanotube. In the case of the semiconducting zigzag nanotube, however, the isolated nitrogen impurity forms a flat energy level lying inside the band gap, 0.2 eV below the bottom of conduction band. It hybridizes with the π orbitals to create a spatially localized state decaying exponentially with an extent of about 20 Å. This singly occupied state is chemically active, and should also be observable using electron spin resonance. We demonstrate the possibility of forming a covalent bond

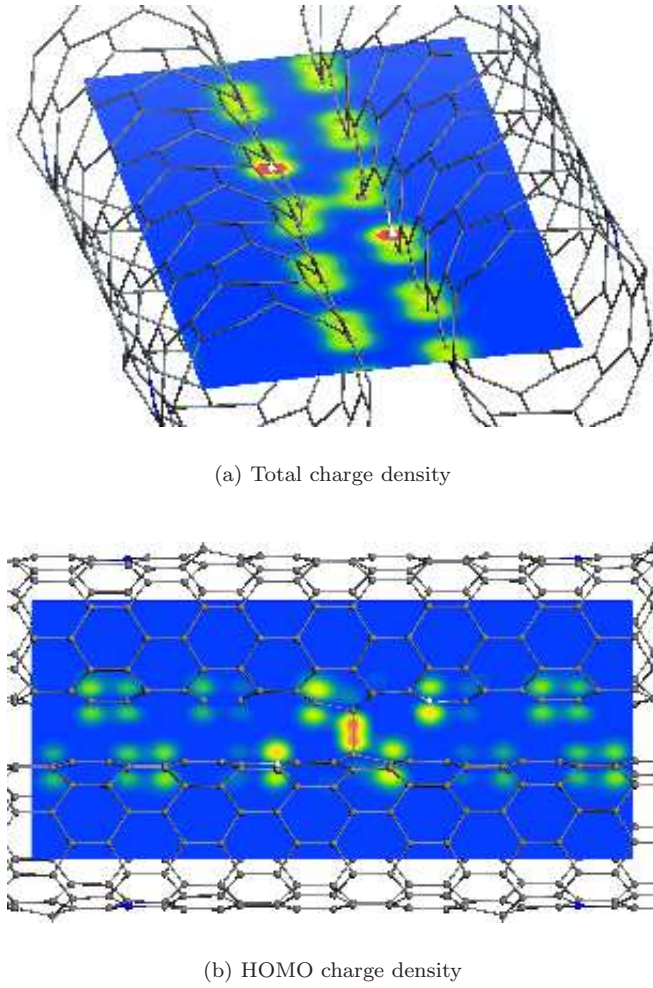


FIG. 3: Two zigzag nanotubes each doped with nitrogen (white balls), facing each other. The chemical bond is formed between the two carbon atoms (grey balls), which have the maximum of the spin density in the isolated nanotube. The slice taken through the C–C bond shows the distribution of the a) total charge density and b) density of the HOMO orbital using the colour map, with blue corresponding to the lowest and red to the highest densities.

between two nanotubes with impurities that face each other. This opens the intriguing general possibility for chemical bonding between suitably doped carbon nan-

otubes or indeed with other ligands. Such tube–tube junctions could be interesting from a device perspective as the intertube bond will probably change the tunneling properties between the tubes considerably. The ligand–binding properties of the localized defect site, of interest in chemical sensing applications, is currently under investigation.

The authors would like to thank Peter Littlewood and Ben Simons for valuable discussions.

- [1] A. Oberlin, M. Endo, and T. Koyama, *Carbon* **14**, 133 (1976); *J. Cryst. Growth* **32**, 335 (1976)
- [2] S. Iijima, *Nature (London)* **354**, 56 (1991).
- [3] R. Saito, G. Dresselhaus, and M.S. Dresselhaus, *Physical Properties of Carbon Nanotubes* (Imperial College Press, London, 1998).
- [4] M. Yudasaka *et al.*, *Carbon* **35**, 195 (1997).
- [5] R. Sen *et al.*, *Chem. Phys. Lett.* **287**, 671 (1998).
- [6] M. Terrones *et al.*, *Appl. Phys. Lett.* **75**, 3932 (1999).
- [7] N. Grobert *et al.*, *Appl. Phys. A* **70**, 175 (2000).
- [8] W. Q. Han, *Appl. Phys. Lett.* **77**, 1807 (2000).
- [9] R. Kurt, J. M. Bonard, and A. Karimi, *Thin Solid Films* **398-399**, 193 (2001); R. Kurt *et al.*, *Carbon* **39**, 2163 (2001).
- [10] R. Czerw *et al.*, *Nano Letters* **1**, 457 (2001).
- [11] M. Terrones *et al.*, *Appl. Phys. A* **74**, 355 (2002).
- [12] S. Trasobares *et al.*, *J. Chem. Phys.* **116**, 1 (2002).
- [13] X. Wang *et al.*, *J. Phys. Chem. B* **106**, 2186 (2002).
- [14] C. J. Lee *et al.*, *Chem. Phys. Lett.* **359**, 115 (2002).
- [15] O. Stephan *et al.*, *Science* **266**, 1683 (1994).
- [16] D. Golberg *et al.*, *Carbon* **38**, 2017 (2000); D. Golberg *et al.*, *Diam. and Related Mater.* **10**, 63 (2001).
- [17] C. C. Kaun *et al.*, *Phys. Rev. B* **65**, 205416 (2002).
- [18] J.-Y. Yi and J. Bernholc, *Phys. Rev. B* **47**, 1708 (1993).
- [19] P. E. Lammert, V. H. Crespi, and A. Rubio, *Phys. Rev. Lett.* **87**, 136402 (2001).
- [20] H. J. Choi *et al.*, *Phys. Rev. Lett.* **84**, 2917 (2000).
- [21] M.C. Payne *et al.*, *Rev. Mod. Phys.* **64**, 1045 (1992).
- [22] V. Milman *et al.*, *Int. J. Quant. Chem.* **77**, 895 (2000).
- [23] J. P. Perdew, K. Burke, and M. Ernzerhof, *Phys. Rev. Lett.* **77**, 3865 (1996);
- [24] W. Andreoni, F. Gygi, and M. Parrinello, *Chem. Phys. Lett.* **190**, 159 (1992).
- [25] G. Csanyi and T. A. Arias, *Chem. Phys. Lett.* **360**, 552 (2002). **78**, 1396(E) (1997).
- [26] M.S. Fuhrer *et al.*, *Science* **288**, 494 (2000).